Electronic Supplementary Information for

Torsional Behaviors of Polymer-infiltrated Carbon Nanotube Yarn Muscles by Atomic Force Microscope†

Cheong Hoon Kwon,[a] Kyoung-Yong Chun,[a] Shi Hyeong Kim,[a] Jae-Hyeok Lee,[b] Jae-Ho Kim,[b] Márcio D. Lima,[c] Ray H. Baughman[c] and Seon Jeong Kim*[a]

[a] Center for Bio-Artificial Muscle and Department of Biomedical Engineering, Hanyang University, Seoul, 133-791, Korea. *E-mail: sjk@hanyang.ac.kr*

[b] Department of Molecular Science and Technology, Ajou University, Suwon, 443-749, Korea.

[c] The Alan G. MacDiarmid NanoTech Institute, University of Texas at Dallas, Richardson, TX 75083, USA.

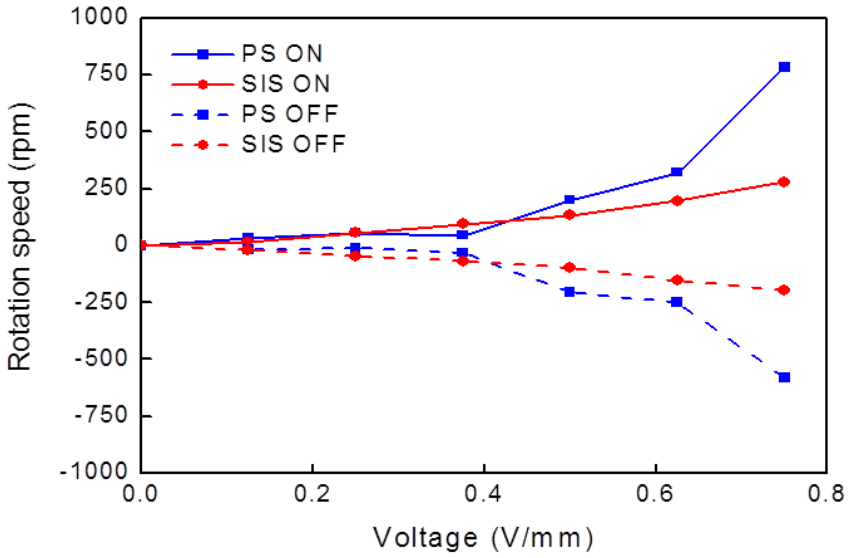

Fig. S1 Rotation speed, revolutions per minute (rpm) changes depending on the voltage for PS-infiltrated CNT and SIS-infiltrated CNT torsional yarn muscles.

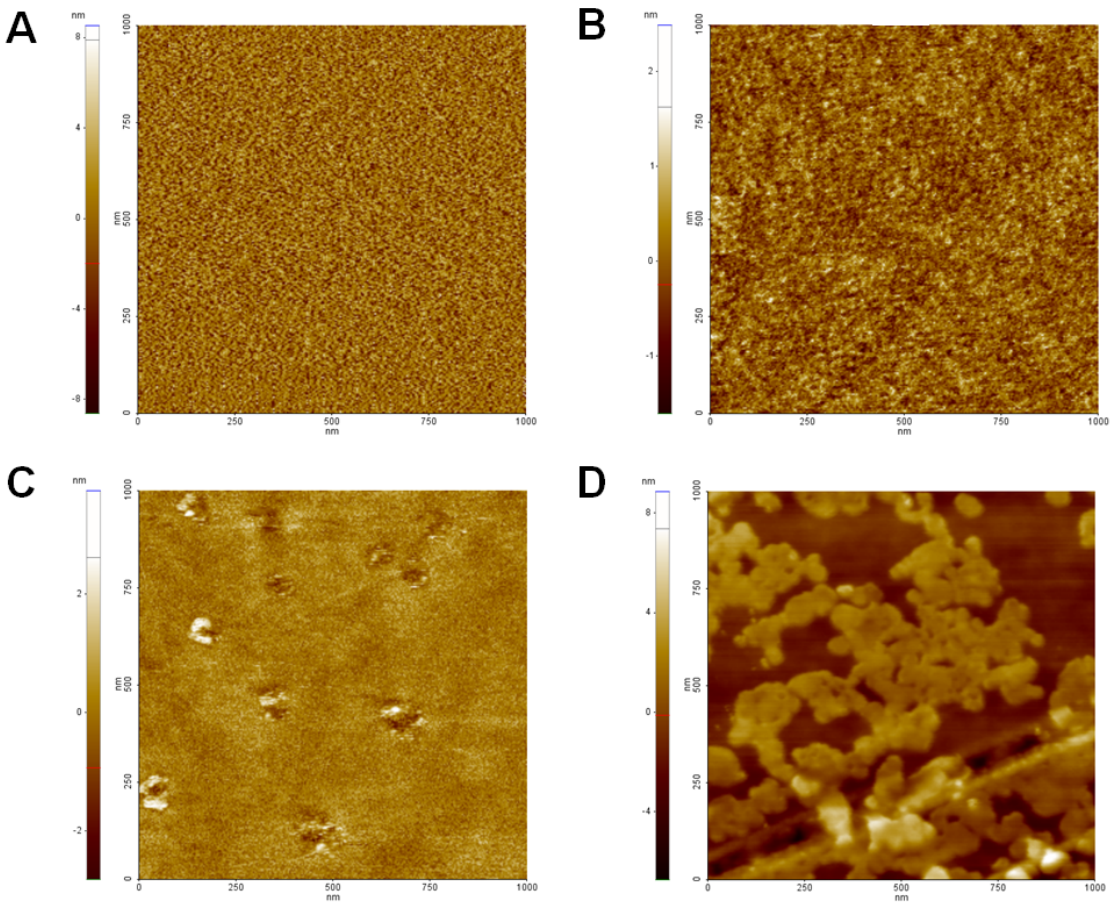

Fig. S2 AFM topographic images of PS as a function of temperature. (A) room temperature, (B) 40 ºC, (C) 80 ºC, and (D) 150 ºC.

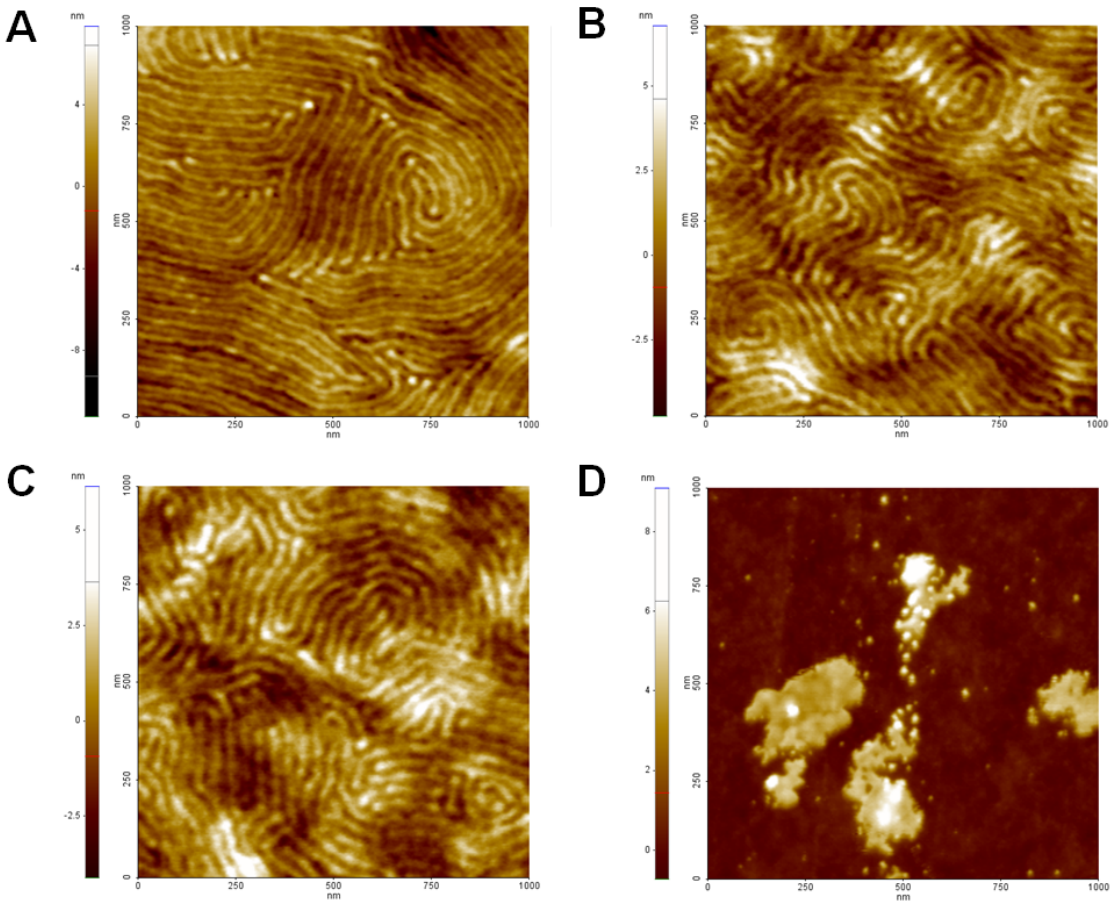

Fig. S3 AFM topographic images of SIS as a function of temperature. (A) room temperature, (B) 40 ºC, (C) 80 ºC, and (D) 150 ºC.

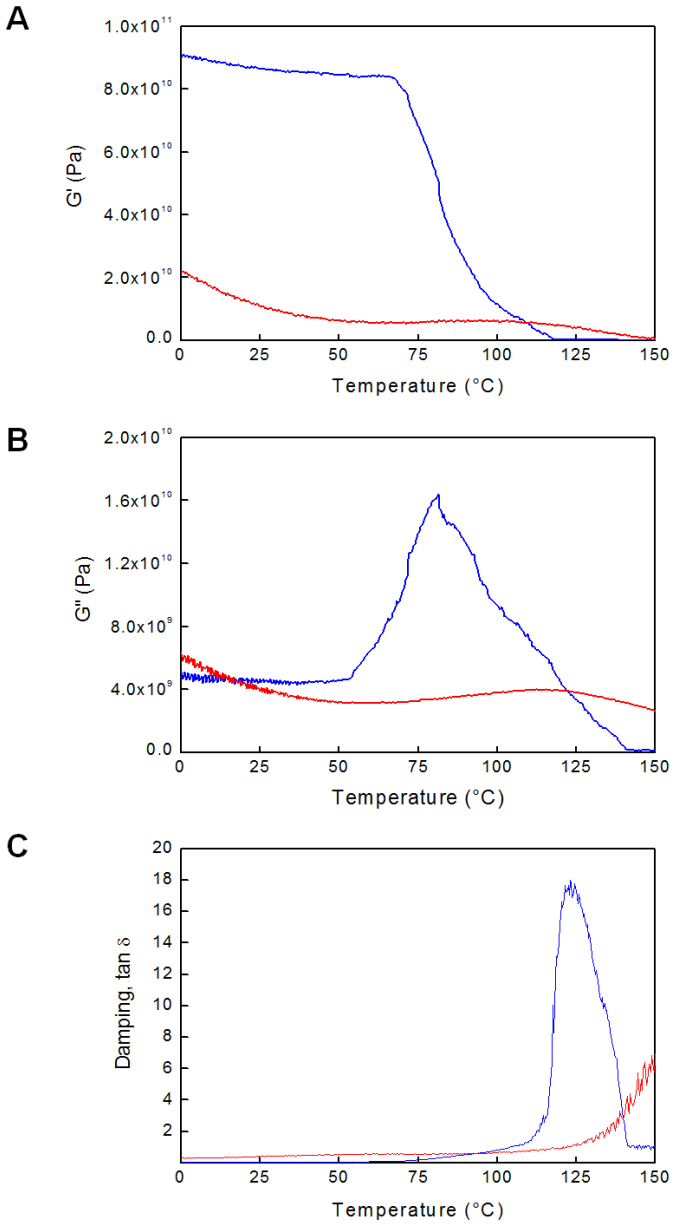

Fig. S4 Dynamic mechanical analyzer results to verify the torsional performance of PS-infiltrated CNT yarn (blue line) and SIS-infiltrated CNT yarn (red line) at 1 Hz. (A) Temperature dependence of storage modulus, G'. (B) Loss modulus, G" for PS and SIS-infiltrated CNT torsional yarn muscles. (C) Tangent δ for PS-infiltrated CNT yarn muscles and SIS-infiltrated CNT torsional yarn muscles.

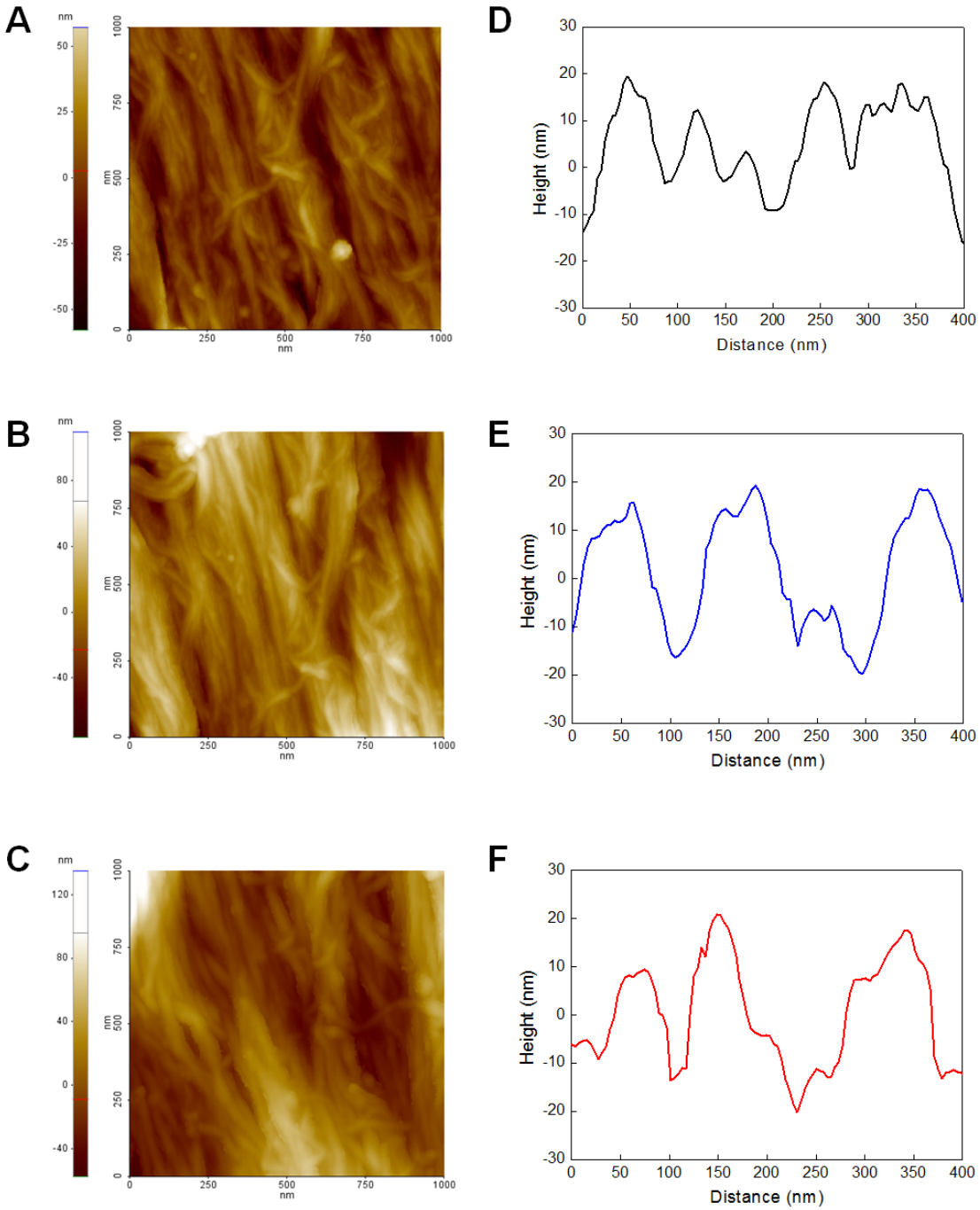

Figure S5. AFM surface morphologies (for 1-μm square grid) of polymer-infiltrated CNT torsional yarn muscles at 25 °C. Topographic images and height distributions for polymer-infiltrated CNT yarns. (A and D) Guest-free CNT yarn. (B and E) PS-infiltrated CNT yarn, (C and F) SIS-infiltrated CNT yarn.